Environ Geol (2008) 56:741–752
DOI 10.1007/s00254-008-1379-9

SPECIAL ISSUE

Sulfation of calcitic and dolomitic lime mortars in the presence of diesel particulate matter

G. Cultrone · A. Arizzi · E. Sebastián · C. Rodriguez-Navarro

Received: 28 March 2008 / Accepted: 8 May 2008 / Published online: 27 May 2008

Abstract The sulfation of four types of calcitic and dolomitic lime mortars exposed to SO_2 in the presence of particulate matter from diesel vehicle exhaust emissions has been investigated. The binders mineralogy and mortars texture are the main factors influencing the formation of deleterious sulfate salts. The type of binder also influences the pore size distribution and the total porosity of the mortars: for equal aggregate (quartz or dolomite), dolomitic lime mortars have smaller pores and higher porosity than calcitic ones. During the first 24 h exposure to SO_2, calcitic lime mortars undergo a higher weight increase than dolomitic ones due to rapid formation of gypsum on their surface. However, at the end of the sulfation test (10 days), dolomitic mortars show a higher weight increase due to massive formation of epsomite and gypsum, which is facilitated by their higher porosity and the high reactivity of Mg phases in the porous and partially carbonated binder. Control samples (not covered with diesel particulate matter) also develop calcium and magnesium sulfates upon long term exposure to SO_2. This is due to the presence of uncarbonated Ca and Mg hydroxides that promote SO_2 fixation as sulfates. However, the amount and size of sulfate crystals are significantly smaller than those observed on samples covered with diesel particulate matter. These results show that diesel particulate matter enhances the sulfation of lime mortars and demonstrate that sulfation of dolomitic lime is an important mechanism for the in situ formation of highly soluble and deleterious hydrated magnesium sulfates (epsomite and hexahydrite). The use of dolomitic limes in the conservation of monuments exposed to air pollution in urban environments may therefore pose a significant risk.

Keywords Dolomitic · Calcitic · Lime mortar · Air pollution · Diesel particulate matter · Sulfation · Gypsum · Epsomite

G. Cultrone (✉) · A. Arizzi · E. Sebastián · C. Rodriguez-Navarro
Department of Mineralogy and Petrology, University of Granada, Granada, Spain
e-mail: cultrone@ugr.es

Introduction

Carbonate rocks have been calcined to produce calcitic and dolomitic limes since the advent of pirotechnology ca. 14,000 years ago (see Elert et al. 2002 and references therein). While calcitic lime is made up of lime (CaO), dolomitic lime (also known as magnesian lime) is composed of a mixture of lime and magnesia (MgO). These oxides are slaked in water to produce calcium and magnesium hydroxides. Afterwards the hydroxides can be mixed with an aggregate to prepare lime mortars and plasters (Boynton 1980). Such building materials were used thoroughly until the discovery of Portland cement in 1824 (Cowper 1927). After its discovery, Portland cement replaced lime as the binder of choice, and attracted a significant amount of research (Rodriguez-Navarro et al. 1998).

Recently, however, the study of lime mortars has gained a renewed interest within the material science community (Rodriguez-Navarro et al. 2005). In parallel, the use of lime-based binders in conservation interventions has been growing steadily. This is due to the greater chemical and physical compatibility of lime-based binders with traditional building materials if compared to Portland cement (Rodriguez-Navarro et al. 1998; Degrise et al. 2002; Genestar and Pons 2002; Maravelaki Kalaitzaki et al. 2003;

Moropoulou et al. 2005). A significant amount of research has thus focused on the analysis of this ancient building material (Elert et al. 2002). For instance, research on the slaking of lime and the evolution of hydrated lime particles upon aging has been performed (Rodriguez-Navarro et al. 1998, 2005). The carbonation of lime mortars and their subsequent hardening (Atzeni et al. 1996; Cazalla et al. 2000; Rodriguez-Navarro et al. 2002; Van Balen 2005; Lawrence et al. 2007) as well as their durability when subjected to different decay processes (Lanas et al. 2006b) have also been studied. The ability of lime mortars to act as a sacrificial layer buffering stone damage during decay processes has been investigated, while attention has been drawn to the possible role of lime mortars in promoting stone decay (Lubelli et al. 2006; Moreno et al. 2006). Despite these research efforts, little is known on the differential weathering behavior of calcitic and dolomitic lime mortars and plasters. Although both types of lime mortars are highly similar in many aspects, the presence of magnesium components brings about some differences related to composition and properties that will have an impact on their weathering behavior and should be studied prior to their use in conservation interventions (Lanas et al. 2006a), specially in polluted urban centers.

Atmospheric pollution and acid deposition on materials is recognized as one of the most important and common causes of decay endangering the built heritage (Winkler 1973; Price 1996; Rodriguez-Navarro and Sebastian 1996; Pérez Bernal and Bello López 2004). Atmospheric pollutants (solid, liquid and gaseous) in urban environments are deposited on sculptures and building materials (stone, mortar and brick) inducing their chemical corrosion and the eventual formation of harmful salts (mainly sulfates). The formation of black crusts (i.e., gypsum crusts) is influenced by the deposition of metallic and carbonaceous particles (Del Monte et al. 1981, 1984). These particles play a critical role in the sulfation of carbonate (e.g., limestone) and non-carbonate (e.g., granites) stones (Rodriguez-Navarro and Sebastian 1996; Simão et al. 2006). In particular, it has been shown that particulate matter from diesel vehicle exhaust, one of the main pollutants in urban environments, is highly effective in catalyzing the fixation of SO_2 as sulfates in the presence of humidity, thus being an important contributor to the sulfation of stone (Rodriguez-Navarro and Sebastian 1996; Simão et al. 2006). Because diesel motor vehicles exhaust emissions are growing steadily worldwide, it is foreseen that their effects on building materials will be exacerbated in the future. It is therefore important to disclose the role of such emissions on the weathering of building materials other than stone.

Many researches describe the effects of SO_2 and other pollutants (e.g., particulate matter) on the decay of stones (Gauri and Holden 1981; Zappia et al. 1992; Sabbioni et al. 1993; Rodriguez-Navarro and Sebastian 1996; Cultrone et al. 2004; Saiz Jiménez et al. 2004). Conversely, little research has focused on the study of the effects of atmospheric pollution on the decay of lime mortars (see review by Yates 2003), and these studies are almost exclusively devoted to calcitic lime mortars (Zappia et al. 1994; Martínez Ramirez et al. 1997, 1998; Sabbioni et al. 1998; Pérez Bernal et al. 2004). Although Niesel and Schimmelwitz (1971) and Hoffmann et al. (1977) suggested that SO_2 plays an important role in the weathering of dolomitic lime mortars, there is no experimental work studying the effects of atmospheric pollution and, in particular, the role of particulate matter, on the sulfation of dolomitic lime mortars, even though these materials have been profusely used worldwide (Vecchio et al. 1993; Bläuer-Böhm and Jägers 1997; Montoya et al. 2003).

Most studies on dolomitic lime mortars have focused either on the comparison of their textural and mechanical properties with those of calcitic lime mortars, or on their carbonation. For instance, Atzeni et al. (1996) pointed to the better mechanical properties presented by mortars containing magnesium over purely calcitic ones. Lanas et al. (2006b) evaluated the strength and pore structure evolution of 180 different magnesian lime-based mortars, and their behavior when subjected to accelerated weathering tests. A number of studies have focused on the analysis of the carbonation of dolomitic lime mortars, which is a more complex process than the carbonation of calcitic lime. On the one hand, reaction of portlandite ($Ca(OH)_2$) with atmospheric CO_2 leads to the formation of calcium carbonate, as in calcitic limes. On the other hand, the carbonation of brucite ($Mg(OH)_2$) results in the formation of amorphous (hydrated) Mg carbonate and/or (metastable) hydrous carbonates including hydromagnesite ($Mg_5(CO_3)_4(OH)_2{\cdot}4H_2O$), dypingite ($Mg_5(CO_3)_4(OH)_2{\cdot}5H_2O$), artinite ($Mg_2CO_3(OH)_2{\cdot}3H_2O$), nesquehonite ($MgCO_3{\cdot}3H_2O$), and lansfordite ($MgCO_3{\cdot}5H_2O$) (Königsberger et al. 1999; Lanas and Álvarez 2004). Additional supply of Ca ions from portlandite dissolution may lead to the precipitation of huntite ($Mg_3Ca(CO_3)_4$) (Königsberger et al. 1999). Formation of the thermodynamically stable magnesite ($MgCO_3$) is kinetically hindered (Lanas and Álvarez 2004): apparently, magnesite forms at high temperature (T) following dehydroxilation of brucite and solid state carbonation (Churakov et al. 2004). Regarding the kinetics of brucite carbonation in air and at room T, it has been shown that this is a very slow process (Atzeni et al. 1996; Lanas et al. 2006a). This typically leads to the persistence of a fraction of non-carbonated brucite over long periods of time (years) (Lanas et al. 2006a).

The interaction of SO_2 with lime mortars may result in the formation of different calcium and magnesium sulfates depending on the composition and textural properties of the

mortar (type of binder and aggregate) and exposure conditions (Yates 2003). In their pioneering work, Hoffmann et al. (1977) studied the differential weathering behavior of calcitic and dolomitic lime mortars exposed to SO_2. They reported high sulfate concentrations in the surface area (about 3 mm thick) which was subjected to flaking off and disintegration in the case of calcitic and dolomitic mortars, respectively. Although this may imply salt crystallization damage, the authors did not investigate the formation of salts nor discussed any damage mechanism (Yates 2003).

Formation of gypsum (and associated crystallization damage) upon exposure of lime mortars to SO_2 has been reported (e.g., Zappia et al. 1994). However, almost no experimental data exist confirming the formation of Mg sulfates upon sulfation of dolomitic limes, although some researchers have pointed to this possibility. For instance, Grodten et al. (1997) indicate that salt weathering of sandstone in ancient buildings could be related to the presence of dolomitic lime mortars. Laue and Siedel (2003) report honeycomb weathering associated to epsomite and hexahydrite crystallization in porous sandstone, suggesting that the Mg could derive from adjacent dolomitic lime mortars and the sulfates could have an atmospheric source. Siedel (2000) reports formation of epsomite on dolomitic lime mortars in a castle in Saxony (Germany).The author concludes that the highly reactive amorphous magnesium carbonate phase formed upon carbonation of brucite might have favored the formation of magnesium sulfate in contact with sulfur compounds. There is also experimental evidence on the formation of epsomite upon interaction of SO_2 with Mg-rich substrates such as dolostone (Tambe et al. 1991). Note that while the low solubility of calcium sulfate limits its weathering capacity, highly soluble magnesium sulfates are among the most deleterious salts affecting monuments and statuary (Goudie and Viles 1997; Juling et al. 2004; Pérez Bernal and Bello López 2004; Ruiz-Agudo et al. 2007a). In fact, the crystallization of magnesium sulfate within porous materials is so damaging that this salt is selected for performing standard accelerated salt weathering tests (ASTM 1997). It is therefore of the outmost importance to elucidate if lime mortars, both ancient ones as well as those currently used for conservation purposes, may or may not develop such deleterious salts upon exposure to polluted environments.

Here, the sulfation of both calcitic and dolomitic lime mortars in a SO_2-rich atmosphere, in the absence and in the presence of particulate matter from diesel vehicle emission has been studied. The aim of this work is twofold: first, to disclose the differences in sulfation behavior between calcitic and dolomitic limes and to correlate them with their mineralogical and textural characteristics, and second, to determine the role of diesel particulate matter on the sulfation of calcitic and dolomitic lime-based mortars. Ultimately, we strive to demonstrate both that diesel particulate matter plays a critical catalytic role in the oxidation of SO_2 to form sulfuric acid in the presence of humidity and that compositional differences between calcitic and dolomitic limes can lead to the formation of different sulfates following reaction with sulfuric acid. These salts, magnesium sulfates in particular, pose a significant danger to cultural heritage. In lieu of the experimental results, recommendations for usage of lime mortars in conservation interventions are outlined.

Materials and methods

Four types of lime mortars were tested under forced sulfation in the presence of diesel particulate matter. Two types of limes, calcitic (C) and dolomitic (D), were used. C lime, is a long-term aged (16 years) lime putty commercialized by "Mazari de Época", a manufacturer from Mollina, Seville (Spain). The mineralogical and textural characteristics of this lime have been reported elsewhere (Cazalla et al. 2000; Rodriguez-Navarro et al. 2002). D lime was prepared in the laboratory from local dolostone (Sub-Betic Jurassic Dolostones, outcropping at SE Granada Basin, Spain). Crushed samples were calcined in an electric oven at 900°C for 3 h. Afterwards, the oxides were slaked in excess deionized water (oxide/water mass ratio of 1/3) to form a putty. The slaking process lasted ca. 3 h reaching a maximum T of $\sim 80^{\circ}$C. The two types of lime putties were mixed with two types of aggregates, quartz (Qtz) and dolomite (Dol). The Qtz aggregate is a standard aggregate supplied by the Instituto Eduardo Torroja (Madrid, Spain), while the Dol aggregate was prepared using the above-mentioned local dolostone. The granulometry of the two aggregates is reported in Table 1. Qtz was selected as a standard, inert aggregate, while Dol was chosen to evaluate the possible role of this aggregate in the formation of magnesium sulfates upon SO_2 exposure. We choose not to use calcite as an aggregate, first because the aggregate masks the formation of calcite upon carbonation, thus preventing a clear evaluation of this process, and second,

Table 1 Grain size distribution of quartz (Qtz) and dolomite (Dol) aggregates

∅ sieve (mm)	Qtz (wt.%)	Dol (wt.%)
2.00	0	0
1.00	36.94	42.74
0.50	32.54	27.81
0.16	22.22	21.99
0.08	8.80	7.46

because this aggregate has been previously used for testing sulfation of lime mortars (Zappia et al. 1994).

Mortars were prepared by manually mixing lime putties and aggregates for 20 min. The chosen binder:aggregate ratio was 1:3 (by volume) because this is considered to be the best for architectural conservation works (Moropoulou et al. 2002). The fresh mortar paste was poured into PVC boxes (2 × 2.5 × 5 cm) and gently compacted. Mortar samples were removed from the boxes 1 week after preparation and subjected to natural carbonation in the laboratory for one year at 18–22°C and relative humidity (RH) of 40 ± 10%. The four groups of mortars prepared were identified as follows: calcitic lime–quartz aggregate (C–Qtz), calcitic lime–dolomite aggregate (C–Dol), dolomitic lime–quartz aggregate (D–Qtz) and dolomitic lime–dolomite aggregate (D-Dol).

A preliminary analysis of the limes and the aggregates was made to identify their composition. The mineralogy of the samples was determined by means of X-ray diffraction (XRD) on a Philips PW1710 diffractometer with an automatic slit, Cu$K\alpha$ radiation, 3° to 60° 2θ explored area and 0.1° 2θ/s goniometer speed. Data were collected and interpreted using the XPowder software package (Martín 2004). The calcitic (C) lime is composed of portlandite with trace amounts of calcite. The presence of calcite is probably due to partial carbonation of portlandite. The XRD pattern of dolomitic lime (D) shows the Bragg peaks of both portlandite and brucite. Trace amounts of calcite are also present in this lime. The Qtz aggregate is composed of quartz with trace amounts of feldspars, and the Dol aggregate is pure dolomite.

Thermogravimetric (TG) analyses (Shimadzu TGA-50H) were carried out in order to determine the amount of water in the lime putties, as well as to quantify the amount of portlandite, brucite and calcite. TG analyses were performed in flushed-air atmosphere (100 ml/min) at a heating rate of 5°C/min, and 25–950°C interval. Figure 1 shows the TG curves (i.e., weight loss vs. T) of the two lime putties. An initial weight loss of ca. 52% occurred in both limes at 110°C due to water evaporation. This weight loss indicates that the lime:water ratio in both limes is ~1:1. At 370°C there is a second weight loss in the dolomitic lime corresponding to the dehydroxilation of brucite. At 470°C the loss of structural water present in portlandite occurred both in the dolomitic and calcitic limes. From weigh loss values, the calculated amount of portlandite in calcitic lime is 90.8 wt.%, while in the dolomitic lime, 44.5 wt.% corresponds to brucite and 47.4 wt.% to portlandite. As expected, the dolomitic lime shows a brucite/portlandite molar ratio of ~1. At $T > 700$°C another weight loss is detected due to calcite decomposition resulting in CO_2 loss. The amount of calcite in calcitic lime and dolomitic lime is 9.2 and 8.1 wt.%, respectively. In summary, TG results are consistent with XRD results, and confirm that the limes were highly pure, fully slaked and with minimal carbonation.

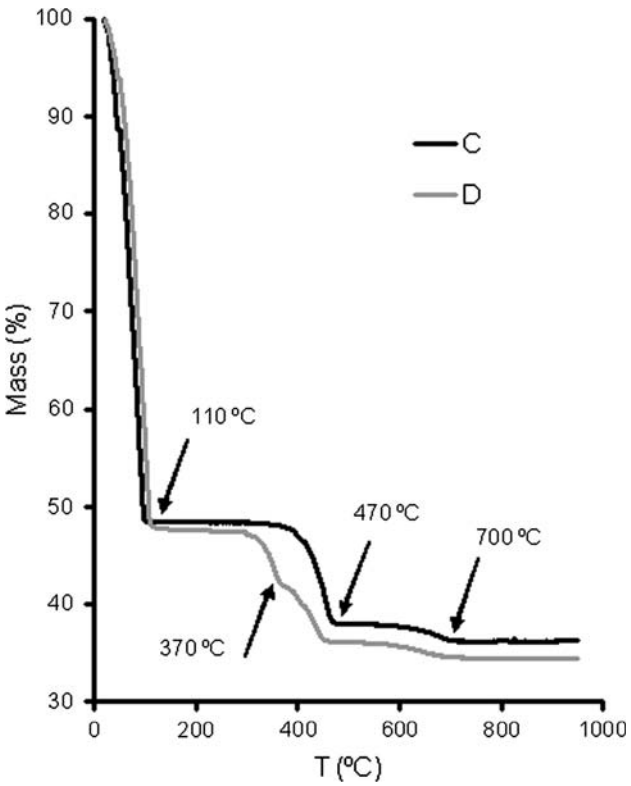

Fig. 1 Thermogravimetric analysis of calcitic (*C*, *black line*) and dolomitic (*D*, *gray line*) lime putties. Temperature (°C) versus weight loss (in %)

The mineralogy and texture of the mortars was studied by means of polarized optical microscopy (OM, Olympus BM-2) equipped with digital microphotography (Olympus DP10). The pore access size distribution and open porosity of the mortars were determined on a Micromeritics Auto-Pore III 9410 mercury intrusion porosimeter (MIP). Freshly cut samples of ca. 2 cm^3 were oven dried for 24 h at 100°C and subsequently analyzed. Two MIP measurements per sample type were made.

Sulfation of the mortar samples (a total of 20; five slabs per mortar type) was performed in a Kesternich chamber (details on the experimental set up have been reported by Rodriguez-Navarro and Sebastian 1996). Four experiments were performed at constant atmospheric pressure (1 atm.), 25°C, ~90% RH and 400 ppm SO_2 concentration over 1, 3, 8 and 10 days. A container full of water was introduced into the chamber to maintain the high RH. Such a high SO_2 concentration, which is ~8,000 times higher than current SO_2 levels in most urban areas (Simão et al. 2006), was selected to obtain a high reaction rate. The tested samples comprised uncovered mortar slabs (control) and samples covered with diesel particulate matter (DPM) that was

directly collected from the mufflers of diesel vehicles using a spatula. DPM was gently and homogeneously sprinkled over the upper surface of the sample with a brush, avoiding the plugging of the mortar pores. Uncovered and DPM covered samples were weighted prior to sulfation test. The average amount of DPM per unit surface of sample was 0.0008 g/cm^2. DPM is mainly composed of poorly crystalline (or amorphous) solids (soot), with elemental carbon (graphite and pregraphitic carbon) as the main component along with organic carbon. Scarce anhydrite and magnetite are also present. A complete study of the mineralogy, morphology and composition of the collected DPM was presented in a previous paper (Simão et al. 2006).

The mineralogy and microtextural features of the mortar samples were characterized before and after sulfation tests by means of field emission scanning electron microscopy (FESEM; Leo Gemini 1530), coupled with an EDX microanalysis (Oxford INCA 200). FESEM secondary electron (SE) images were acquired using small (5 × 5 × 3 mm in size) carbon coated samples.

Weight changes due to sulfate crystallization were determined with A and D ER-120A scales with an accuracy of ±0.0001 g (up to 120 g). Samples were weighed after collection from the Kesternich chamber at predetermined time intervals (1, 3, 8 and 10 days).

N_2 sorption isotherms were obtained at 77 K on a Micromeritics Tristar 3000 under continuous adsorption conditions. Prior to measurement, powder samples were heated at 200°C for 2 h and outgassed to 10^{-3} Torr using a Micromeritics Flowprep. BET analysis (Brunauer et al. 1938) was used to determine the total specific surface area (SSA). The slaked dolomitic lime has a specific surface area of 20.9 m^2/g, while the slaked calcitic lime has a reported surface area of 10.8 m^2/g (Rodriguez-Navarro et al. 2002).

Results and discussion

Mineralogy and texture of lime mortars

As expected, XRD analyses showed that quartz and dolomite were the main mineral phases in C and D lime mortars after 1 year carbonation in air (Fig. 2). Calcite Bragg peaks were present in all XRD diagrams, thus confirming that carbonation of portlandite has occurred. However, carbonation was not complete after one year as indicated by the small Bragg peaks of portlandite and brucite (Fig. 2). It has been reported that even if the carbonation process seems complete, an amount of uncarbonated lime may typically be retained in lime mortars after many years (Cowper 1927; Cultrone et al. 2005; Lawrence et al. 2006). Small Bragg peaks corresponding to lansfordite were detected in the XRD patterns of dolomitic lime mortars. However, superposition of several Bragg peaks of other phases such as portlandite, brucite, calcite, and the aggregate (either dolomite or quartz) on those of lansfordite prevented the unambiguous identification of this phase (as well as any other crystalline magnesium carbonate hydrate). Therefore, its presence was not clearly proved. Lanas and Álvarez (2004) have reported on the difficulty of detecting magnesium carbonate phases following long term carbonation of dolomitic mortars. The authors conclude that only under very specific conditions such as high CO_2 concentration and/or high *T,* nesquehonite or hydromagnesite can develop. Siedel (2000) indicates that no Mg carbonates could be detected in ancient dolomitic mortars (theoretically fully carbonated) using XRD. However, thermal analysis showed the distinctive endothermic peak at 500–575°C of hydrous magnesium carbonates. The author concludes that amorphous magnesium carbonate hydrate is the main end-product of brucite carbonation. Thus, it is highly probable that amorphous magnesium carbonate hydrate formed in D–Qtz and D–Dol mortars. However, due to its amorphous nature, it could not be detected with XRD. In fact, the formation of amorphous magnesium carbonate hydrate may explain the significant reduction in the intensity of brucite Bragg peaks after 1 year carbonation in air; i.e., the intensities of the main Bragg peaks of portlandite and brucite are very similar after 1 year carbonation (Fig. 2). The formation of metastable, and thus highly reactive, amorphous magnesium carbonate may have a direct impact on the sulfation of dolomitic lime mortars, as suggested by Siedel (2000).

Optical microscopy observations (Fig. 3) showed that the union between binder and aggregate was continuous and complete. These observations indicate that the mortars are well cemented. The morphology of Qtz grains ranged from sub-angular to round while Dol grains were subangular. The matrix was micritic. The pores were irregular in shape, with main sizes about 50–100 μm. These large pores were more abundant in dolomitic lime mortars. The differences in porosity and pore entry size distribution (PSD) of calcitic and dolomitic lime mortars were clearly defined with MIP. All mortars showed a bimodal PSD (Fig. 4). The larger pores (with size in the range 10–100 μm) appear to be related with the type of aggregate, because this PSD maximum did not change with the lime type. In fact, pores with $r > 10$ μm are controlled by packing of the aggregate. Qtz aggregate leads to monodisperse macropores because of its rounded shape, while the subangular shape of Dol aggregate results in a wider distribution of pore size for the range 10–50 μm (note that both aggregates have a similar granulometry). The smaller PSD maxima changed depending on the type of binder. Dolomitic lime mortars showed a higher amount of smaller

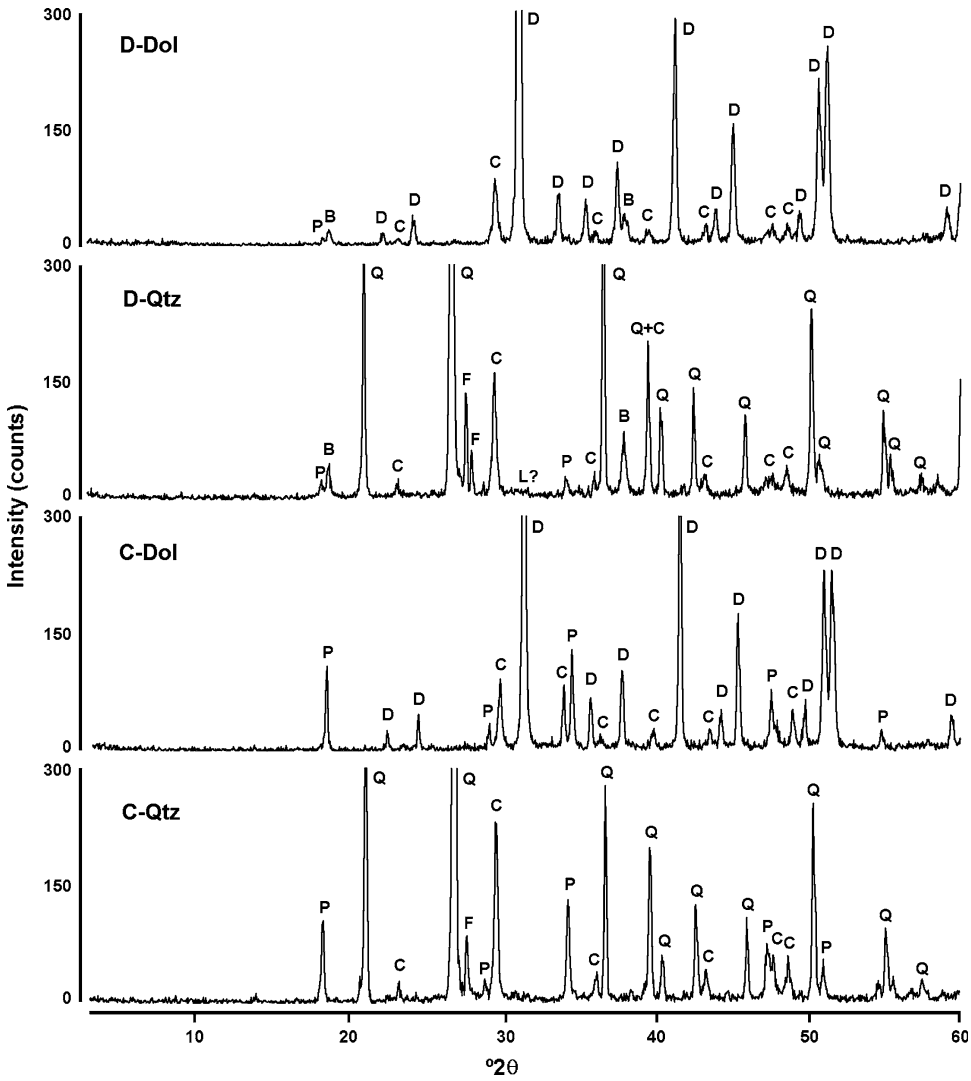

Fig. 2 XRD patterns of calcitic (*C*) and dolomitic (*D*) lime mortars with quartz (*Qtz*) and dolomite (*Dol*) aggregate after 1 year carbonation. Legend: *D* dolomite, *C* calcite, *Q* quartz, *P* portlandite, *B* brucite, *L?* possibly lansfordite

pores, with a PSD maximum at ca. 0.04 μm. Calcitic lime mortars showed a maximum for the smaller pores at around 0.5 μm. Table 2 confirms the textural observations: dolomitic lime mortars are more porous than calcitic lime mortars. Table 2 also shows that dolomitic limes have higher pore area values (S). Apparent and bulk densities (ρ_a and ρ_r) are typical of these types of materials and are clearly higher when the aggregate is dolomite instead of quartz.

The textural differences between the calcitic and dolomitic lime mortars can be explained considering both the differences in particle size and in the carbonation behavior of the two lime types. The higher SSA of dolomitic lime is associated to a smaller particle size. Such a smaller particle size facilitates a denser packing of the hydroxide crystals in the mortar matrix. This denser packing will lead to smaller pores than in the case of calcitic lime. On the other hand, carbonation results in a reduction of porosity due to the differences in molar volume between hydroxides and carbonates (Cazalla et al. 2000). Therefore, because the rate of carbonation of calcitic lime is higher than that of dolomitic lime (Boynton 1980), dolomitic lime mortars will undergo a lower reduction in porosity after 1 year curing time. The more thorough carbonation of calcitic lime mortars resulted in plugging of the smallest pores and the displacement of the smaller-size PSD maximum towards larger pore sizes. Note that calcitic limes carbonate because of portlandite transformation into calcite. In dolomitic lime, only a part of its mass is composed of portlandite and turns into calcite. The other phase, brucite, does not easily carbonate (see Lanas et al. 2006a and references therein). In fact, the development of hydrated magnesium carbonate phases is complex and is influenced by pH, CO_2 concentration and temperature during carbonation process (Lanas and Álvarez 2004; Lanas et al. 2006b). Limited carbonation in dolomitic lime mortars may have therefore prevented the plugging of the smaller pores and limited the associated porosity reduction, as shown by MIP results.

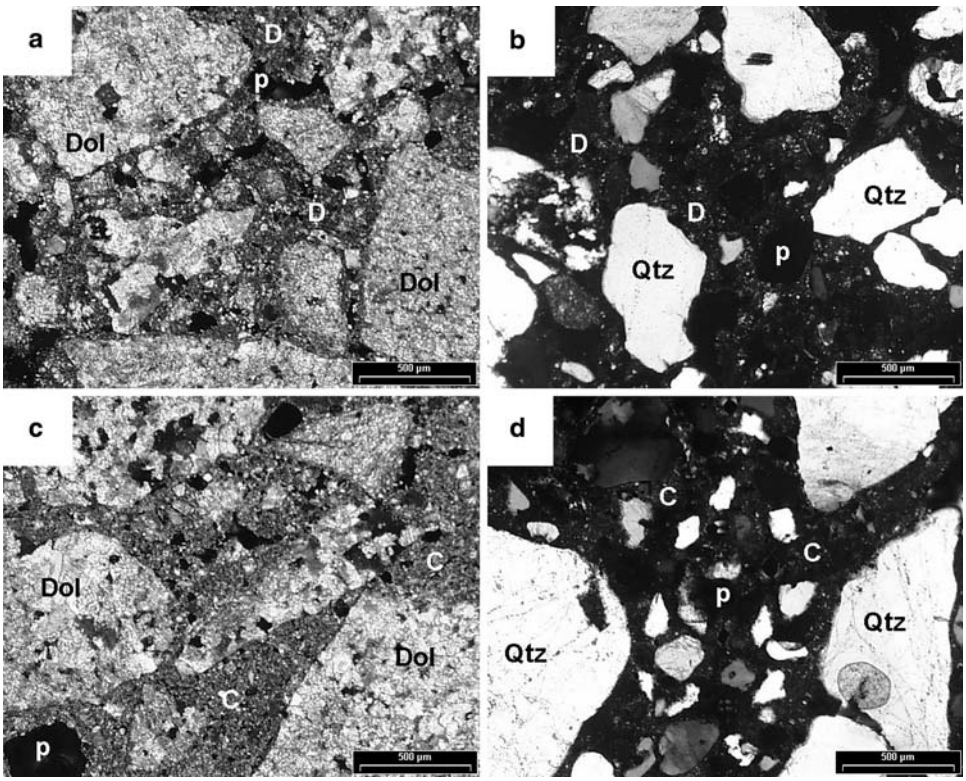

Fig. 3 Optical-microscope microphotographs of D–Dol (**a**), D–Qtz (**b**), C–Dol (**c**) C–Qtz (**d**) mortars. Legend: *D*: dolomitic lime matrix, *C* calcitic lime matrix, *Dol* dolomite aggregate, *Qtz* quartz aggregate, *p* pore

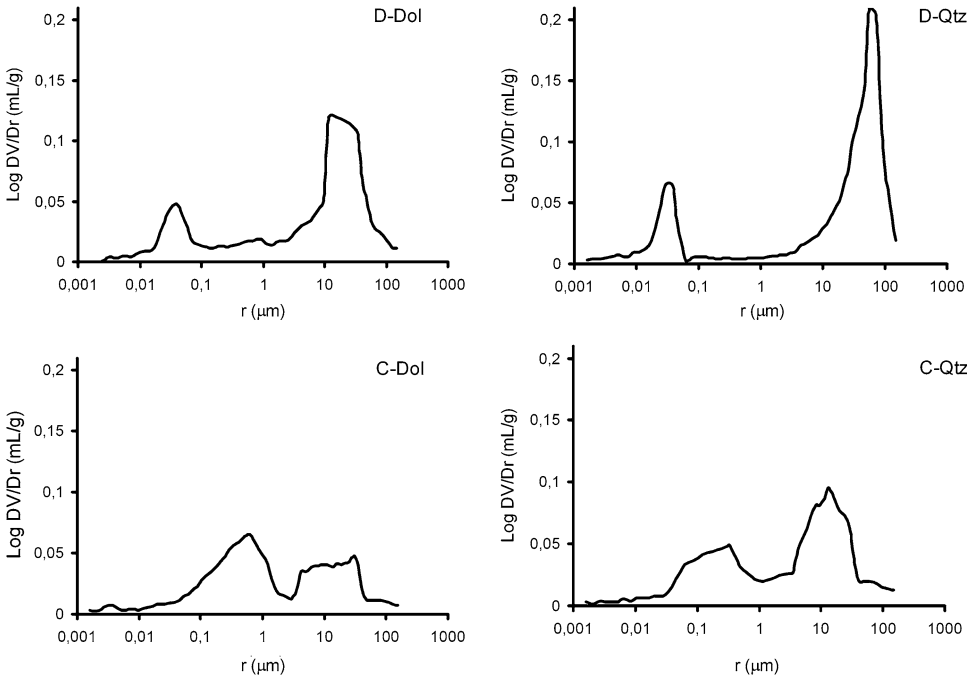

Fig. 4 MIP pore size distribution curves [i.e. log differential intruded volume (mg/l) vs. pore radius (μm)] of dolomitic (D–Dol, D–Qtz) and calcitic (C–Dol, C–Qtz) lime mortar samples

Formation of sulfates upon SO_2 attack

FESEM observations revealed the formation of newly formed mineral phases in DPM-free mortars as well as in samples covered with DPM. Differences in the composition and amount of newly formed phases depended on exposure time and type of mortar tested. It is interesting to notice that new mineral phases crystallized on all mortars covered with DPM after just 24 h SO_2 exposure. While only gypsum ($CaSO_4{\cdot}2H_2O$) developed on calcitic lime mortars, epsomite ($MgSO_4{\cdot}7H_2O$), in addition to gypsum, developed on dolomitic ones. Gypsum crystals generally presented a rosette shape (Fig. 5a) which suggests the rapid precipitation of numerous and small $CaSO_4{\cdot}2H_2O$ crystals. Such

Table 2 Porosimetric parameters of lime mortars

	S	ρ_a	ρ_r	P
D–Dol	3.03	2.03	2.80	27.34
D–Qtz	4.71	1.88	2.65	29.28
C–Dol	3.16	2.01	2.66	24.61
C–Qtz	2.74	1.94	2.71	28.46

S total pore area (m^2/g), ρ_a apparent density (g/cm^3), ρ_r real density (g/cm^3), P porosity (%)

features are typical of crystallization at a high supersaturation (Sunagawa 1981). In some cases, these rosettes coalesced forming large gypsum plates (Fig. 5b, c). Epsomite crystals (see Fig. 5d and EDX microanalysis in inset) showed the typical dehydration cracks described by Ruiz-Agudo et al. (2007b) Presumably, these cracks developed due to vacuum dehydration undergone during sample preparation (carbon coating) and/or in the FESEM chamber. During the first day of SO_2 exposure, the surface of mortar samples showed areas free from gypsum and/or epsomite (Fig. 5b). Such areas corresponded to large aggregate grains (either quartz or dolomite) with no sign of corrosion. Apparently, the sulfation is restricted to the highly reactive matrix (carbonated and uncarbonated binders), the aggregates thus playing no active role in this process. After 10 days SO_2 exposure, mortar surfaces were fully covered by a crust of gypsum, plus epsomite and/or hexahydrite (in the case of the dolomitic lime mortars) (Fig. 5e). While epsomite still maintains, although cracked, its habit, hexahydrite shows its typical "corroded" morphology (Ruiz-Agudo 2007). The morphology of gypsum crystals was different after 10 days SO_2 exposure: instead of the "rosette" shape, crystals were prismatic; i.e., {010} forms were clearly recognizable (Fig. 5f). Such a habit change is probably due to gypsum crystallization at a lower supersaturation during the final stages of the sulfation test. Note that the morphology of gypsum is affected by free sulfate content and supersaturation (Rodriguez-Navarro and Doehene 1999; Abdel Aal et al. 2004; Titiz Sargut et al. 2007). Control samples also showed the development of gypsum and epsomite crystals (Fig. 5g). However, sulfate crystals were only clearly detected after 10 days exposure to SO_2, and at this time their size and abundance were significantly lower than those of samples covered with DPM.

Samples covered with DPM showed a significant weight gain over the course of the sulfation test due to the formation of Ca and Mg sulfates (Fig. 6). Weight gains were nearly identical in samples prepared with the same lime type but with different aggregate. These results confirm that the tested aggregates have no significant influence in the kinetics and degree of sulfation. Conversely, two different trends in weight gain were observed in samples covered with DPM that depended on the type of lime and the length of SO_2 exposure (Fig. 6). During the first 24 h, mortar samples prepared with calcitic lime showed a higher weight increase than those prepared with dolomitic lime. However, from day 1 till day 10, dolomitic lime mortar samples experienced a higher weight gain. The higher Ca content in calcitic lime may have favored the rapid generation of gypsum crystals, thus explaining the initial higher rate of weight increase experienced by calcitic lime mortars. Initially, the reaction should have been restricted to the surface of the mortars, but after 3, 8 and 10 days it appears that a significant volume of the samples was involved in the precipitation of sulfate crystals. Considering that dolomitic lime mortars are more porous (see Fig. 4; Table 2), SO_2 diffusion through the pore network should have been facilitated during this second stage of the sulfation process. In addition, the higher amount of smaller pores in dolomitic lime mortars may have favored capillary water condensation, thus enhancing the adsorption, oxidation—mediated by particulate matter—and hydrolysis of SO_2, as well as the dissolution of Mg and Ca phases (carbonates and hydroxides) in the binder. Overall, these factors resulted in a higher yield of sulfate precipitation in the dolomitic lime mortars upon long term exposure to SO_2. On the other hand, the higher molecular weight (26.8% higher) of epsomite if compared with gypsum may also account for the higher weight increase experienced by dolomitic lime mortars.

Interestingly, control samples (uncovered with DPM) also experienced a weight increase. At the end of the sulfation test, dolomitic lime mortar control samples showed an average weight increase (per unit surface area exposed to SO_2) of 0.036 g/cm^2. This weight increase is 39% lower than that experienced by dolomitic lime mortars covered with DPM. Calcitic lime mortars underwent a weight increase of 0.024 g/cm^2 on average. This value is 12% lower than that of calcitic lime mortars covered with DPM. These results demonstrate that sulfation occurs in the absence of particulate matter, yet they also show that DPM enhances the sulfation of lime mortars.

Both metallic particles (specially those Fe-rich) and nanometer sized carbon-particles (soot) in DPM have been experimentally shown to play a catalytic role in the oxidation of SO_2 to form SO_3 which, in the presence of H_2O, hydrolyzes to form H_2SO_3 and finally H_2SO_4 (Rodriguez-Navarro and Sebastian 1996; Simão et al. 2006). In the case of the lime mortars, the sulfuric acid thus generated can attack the highly reactive newly formed carbonates in the mortars, namely calcite and, in the case of dolomitic lime, also lansfordite and (amorphous) magnesium carbonate hydrate. This latter metastable phase, probably colloidal, should be especially prone to dissolution (Siedel 2000).

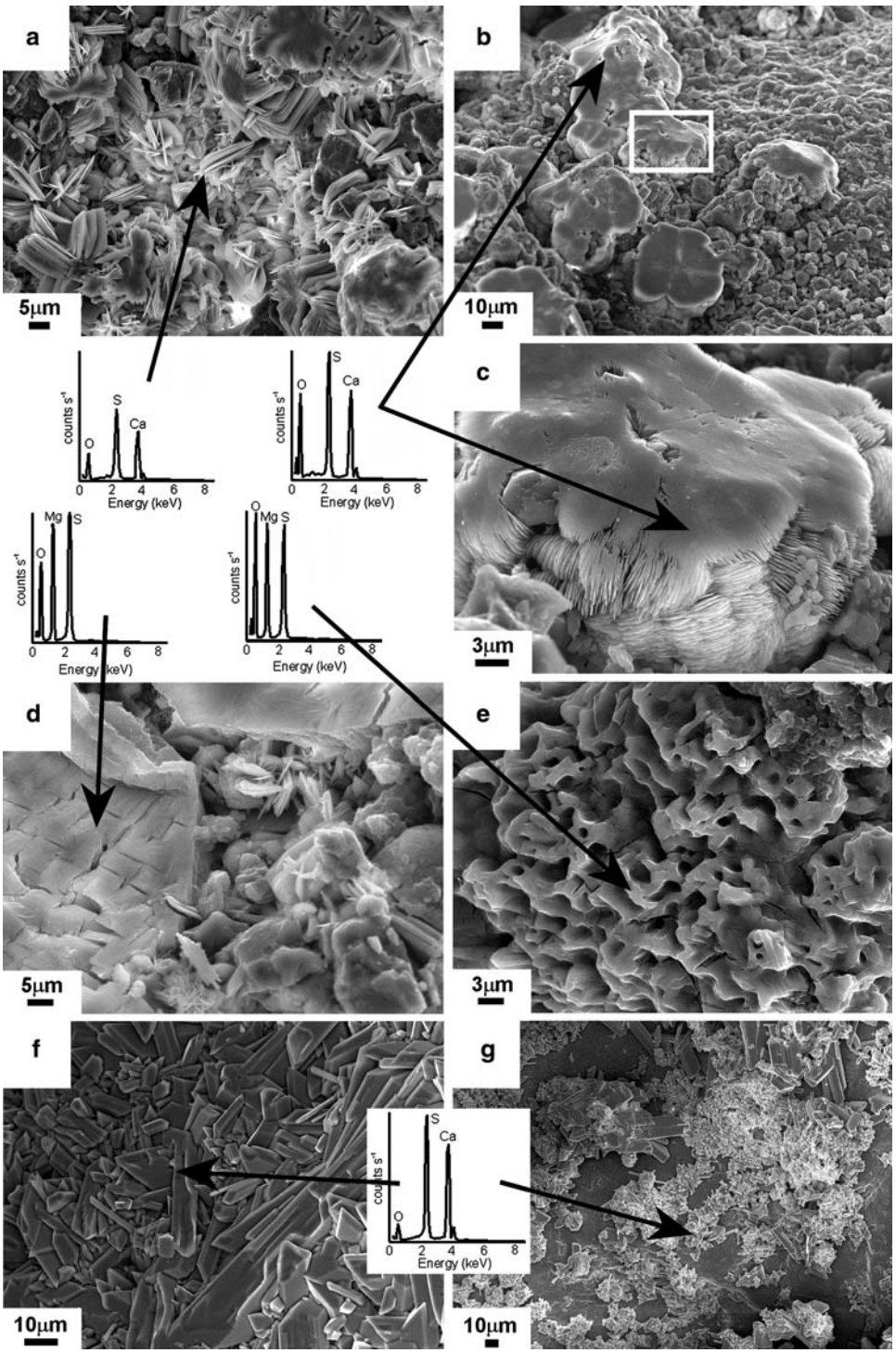

Fig. 5 FESEM images and EDS analyses of aged lime mortars subjected to SO_2 exposure: **a** gypsum crystals with "rosette" morphology in D–Dol mortar after 1 day exposure; **b** gypsum plates in a D–Qtz mortar; **c** detail of the previous image (*white rectangle*) in which gypsum plates are composed of laminar, rosette-like crystals; **d** epsomite crystal in D–Dol mortar after 24 h exposure: note the cracks associated to dehydration; **e** magnesium sulfate crystal with "corroded surface", probably hexahydrite, in D–Qtz mortar after 10 days exposure; **f** development of an uniform crust made of tabular gypsum crystals in C–Dol mortar after 10 days exposure; and **g** presence of a non-uniform gypsum plus Mg sulfate crust on a DPM-free D–Qtz mortar after 10 days exposure. EDX spectra of the different phases are presented in *insets*

Ultimately, the dissolution of Ca and Mg ions in a sulfate-rich solution leads to the precipitation of gypsum and, afterwards, epsomite.

The presence of uncarbonated $Ca(OH)_2$ in calcitic and dolomitic limes mortars, and of $Mg(OH)_2$ in the latter ones, also appears to play a critical role in the fixation of SO_2 as sulfates, as shown by the formation of gypsum and epsomite on the DPM-free control samples. Acid gases are readily absorbed and neutralized in lime hydrate suspensions (Boynton 1980). Dissolution of the hydroxides in the mortars capillary water will lead to alkalinization (pH 10.5–12.4). Such alkaline conditions favor SO_2

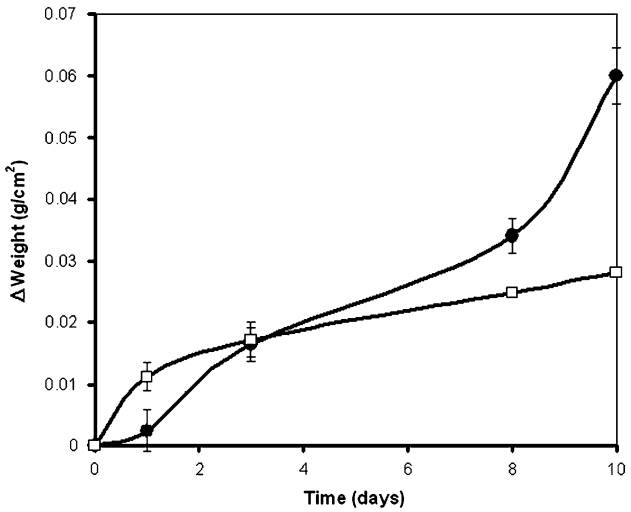

Fig. 6 Weight gain of calcitic (*filled circle*) and dolomitic (*open square*) DPM coated mortar samples versus SO_2 exposure time. Weight gain values have been normalized by the exposed surface area of mortar samples. Average values are presented for each lime type. Error bars indicate standard deviation

dissolution, oxidation and hydrolysis to form sulfite and, ultimately, sulfate ions as follows (Kakaraniya et al. 2007):

$$SO_2 + 2OH^- \rightarrow SO_3^{2-} + H_2O \quad (1)$$

$$SO_2 + SO_3^{2-} + H_2O \rightarrow 2HSO_3^- \quad (2)$$

$$HSO_3^- + OH^- \rightarrow SO_3^{2-} + H_2O \quad (3)$$

$$SO_3^{2-} + 2OH^- \rightarrow SO_4^{2-} + H_2O \quad (4)$$

In the presence of Ca and Mg ions in solution, precipitation of gypsum and epsomite will eventually take place.

Note that alkaline slurries of both calcium and magnesium hydroxide have been thoroughly used (at an industrial-scale) for flue gas desulfurization; i.e., the so-called wet SO_2 scrubbing. However, magnesium hydroxide gives a higher scrubbing capacity because of the more soluble initial reaction product magnesium sulfite, relative to the corresponding calcium salt (Kakaraniya et al. 2007). This latter effect seems to have contributed to the higher sulfation capacity of dolomitic lime mortars if compared with calcitic ones.

Considering that full carbonation of lime mortars is only achieved after long term exposure (years), sulfation in polluted environments will be an active process facilitated by the high alkaline conditions resulting from the dissolution of unreacted hydroxides within capillary water. This process will occur even if particulate matter is not deposited on these materials. Nonetheless, particulate matter would accelerate and promote sulfation of lime mortars.

Conclusions

Calcitic and dolomitic lime mortars suffer decay due to sulfation in a SO_2-rich atmosphere and in the presence of diesel particulate matter emitted by motor vehicles. There are, however, some differences regarding the amount, type, morphology and development of newly formed sulfates depending on the type of lime used.

Higher amounts of sulfates formed in dolomitic mortars if compared to calcitic mortars. The higher reactivity of the former mortars is associated to their higher porosity which favor SO_2 diffusion within pores, and to the larger amount of pores with radius <0.1 μm. The latter pores promote capillary condensation of H_2O, thus enhancing dissolution of Ca and Mg phases (hydroxides and newly formed carbonates) and SO_2. This results in the crystallization of larger amounts of sulfates that in the less porous, less reactive calcitic lime matrix.

While only gypsum crystals develop in calcitic lime mortars, gypsum plus epsomite and hexahydrite crystallize in dolomitic lime mortars. The morphology of gypsum crystal varies depending on $[Ca^{2+}]$ and $[SO_4{}^{2-}]$ concentrations in the pore water. The initial high supersaturation associated to large amounts of Ca^{2+} from dissolution of portlandite and calcite in the binder, results in the development of gypsum with rosette morphologies. Afterwards, consumption of the Ca (originated from calcite and portlandite dissolution), and reduction of $[Ca^{2+}]$ in the pore solution leads to lower supersaturation and the formation of equilibrium shaped, larger gypsum {010} prisms. No similar evolution in the morphology of magnesium sulfates is observed, which implies that the Mg source (uncarbonated brucite plus magnesium carbonates) is not consumed over the time span of the sulfation test.

The aggregates do not influence the development of sulfates during the sulfation test carried out in this research.

The high alkaline conditions resulting from dissolution of uncarbonated Ca and Mg hydroxides in the pore water of the mortars promote the absorption of gaseous SO_2 and its transformation into sulfates. In this respect, Mg hydroxide has a higher absorption capacity than Ca hydroxide. As a result, higher amounts of sulfates are formed in dolomitic lime mortars that in calcitic ones.

It has been observed that the sulfation of lime mortars is enhanced by the presence of diesel particulate matter which acts as a catalyzer for SO_2 oxidation and hydrolysis to form sulfuric acid, which afterwards leads to chemical weathering of the mortars.

This work for the first time shows the close relationship between formation of deleterious magnesium sulfate salts and the attack of dolomitic lime mortars in SO_2 polluted environments. These experimental results help to explain the ubiquitous presence of magnesium sulfate salts

(epsomite and hexahydrite) and the damage associated to their crystallization in many historical buildings where dolomitic limes were used.

Finally, these results demonstrate that the use of repair dolomitic lime mortars in architectural conservation interventions could pose a significant risk associated to the formation of magnesium sulfates in polluted environments.

Acknowledgments This work has been financially supported by the Spanish Government under contract MAT2006-00578, and the research group NRM-179 (Junta de Andalucía, Spain). We thank the personnel of the CIC (UGR) for their help with FESEM and TG analyses.

References

Abdel Aal EA, Rashad MM, El Shall H (2004) Crystallization of calcium sulphate dihydrate at different supersaturation ratios and different free sulphate concentrations. Cryst Res Technol 39:313

ASTM C88-90 (1997) Standard test method for soundness of aggregate by use of sodium sulfate or magnesium sulfate. Annual Book of ASTM Standard 4.2, pp 37–42

Atzeni C, Massidda L, Sanna U (1996) Magnesian limes. Experimental contribution to interpreting historical data. Sci Tech Cult Herit 5:29–36

Bläuer-Böhm C, Jägers E (1997) Analysis and recognition of dolomitic lime mortars. In: Béarat H, Fuchs M, Maggetti M, Pounier D (eds) Roman wall painting: materials, techniques, analysis and conservation. Proceedings of the international workshop. Fribourg, Switzerland, pp 223–235

Boynton RS (1980) Chemistry and technology of lime and limestone. Wiley and Sons, New York

Brunauer S, Emmett PH, Teller E (1938) Adsorption of gases in multimolecular layers. J Am Chem Soc 60:309–319

Cazalla O, Rodriguez Navarro C, Sebastián E, Cultrone G, de la Torre MJ (2000) Aging of lime putty: the effect on traditional lime mortar carbonation. J Am Ceram Soc 83:1070–1076

Churakov SV, Ianuzzi M, Parrinello M (2004) Ab initio study of dehydroxilation–carbonation reaction on brucite surface. J Phys Chem B 108:11567–11574

Cowper AD (1927) Lime and lime mortars. Donhead, London; reprinted in 1998 by the Building Research Establishment Ltd, London

Cultrone G, Rodriguez-Navarro C, Sebastián E (2004) Limestone and brick decay in simulated polluted atmosphere: the role of particulate matter. Air Pollution and Cultural Heritage. Balkema, Amsterdam, pp 141–145

Cultrone G, Sebastián Pardo E, Ortega Huertas M (2005) Forced and natural carbonation of lime-based mortars with and without additives: mineralogical and textural changes. Cement Concrete Res 35:2278–2289

Degrise P, Elsen J, Waelkens M (2002) Study of ancient mortars from Sagalassos (Turkey) in view of their conservation. Cement Concrete Res 32:1457–1463

Del Monte M, Sabbioni C, Vittori O (1981) Airborne carbon particles and marble deterioration. Atmos Environ 15:645–652

Del Monte M, Sabbioni C, Vittori O (1984) Urban stone sulphation and oil-fires carbonaceous particles. Sci Total Environ 36:369–376

Elert K, Rodriguez-Navarro C, Sebastian Pardo E, Hansen E, Cazalla O (2002) Lime mortars for the conservation of historic buildings. Stud Conserv 47:62–75

Gauri KL, Holden GC (1981) Pollutant effects on stone monuments. The outcome can be predicted with reasonable certainty. Environ Sci Tech 15:386–390

Genestar C, Pons C (2002) Ancient covering plaster mortars from several convents and Islamic and Gothic palaces in Palma de Mallorca (Spain). Analytical characterisation. J Cult Herit 4:291–298

Goudie AS, Viles HA (1997) Salt weathering hazards. Wiley, London

Grodten T, Steiger M, Dannecker W (1997) Effect of dolomite-containing mortar on the weathering of mottled sandstone—presentation of an application-related research method. In: Proceedings of the 13th internationale Baustofftagung, Weimar, vol 2, pp 959–965

Hoffmann D, Schimmelwitz P, Rooss H (1977) Interaction of sulfur dioxide with lime plasters. In: Proceedings of the 2nd international symposium on the deterioration of building stones, Athens Nat. Techn. University, Athens

Juling H, Kirchner D, Brüggerhoff S, Linnow K, Steiger M, El Jarad A, Gülker G (2004) Salt damage of porous materials: a combined theoretical and experimental approach. In: Kwiatkowski D, Löfvendahl R (eds) 10th International congress on deterioration and conservation of stone, vol 1. Stockholm (Sweden), pp 187–194

Kakaraniya S, Kari C, Verma R, Mehra A (2007) Gas absorption in slurries of fine particles: SO_2–Mg(OH) 2-$MgSO_3$ system. Ind Eng Chem Res 46:1904–1913

Königsberger E, Königsberger LC, Gamsjäger H (1999) Low-temperature thermodynamic model for the system Na_2CO_3–$MgCO_3$–$CaCO_3$–H_2O. Geochim Cosmochim Acta 63:3105–3119

Lanas J, Álvarez JL (2004) Dolomitic lime: thermal decomposition of nesquehonite. Thermochim Acta 421:123–132

Lanas J, Pérez Bernal JL, Bello MA, Álvarez JI (2006a) Mechanical properties of masonry repair dolomitic lime-based mortars. Cement Concrete Res 36:951–960

Lanas J, Sirera R, Alvarez JI (2006b) Study of the mechanical behavior of masonry repair lime-based mortars cured and exposed under different conditions. Cement Concrete Res 36:961–970

Laue S, Siedel H (2003) Alveolarverwitterung der Sandsteine an der Dorfkirche Leuba, Teilbericht: Gesteinsmaterial, Verwitterung und Salzbelastung. Abschlussbericht der Deutschen Bundesstiftung Umwelt, AZ 18727: Entwicklung einer Technologie zur Restaurierung umweltbedingter Schäden durch Alveoloarverwitterung an Sandsteinen am Beispiel der Dorfkirche Leuba, Deutsche Bundesstiftung Umwelt, 34 S., Osnabrück

Lawrence RMH, Mays TJ, Walker P, D'Ayala D (2006) Determination of carbonation profiles in non-hydraulic lime mortars using thermogravimetric analysis. Thermochim Acta 444:179–189

Lawrence RMH, Mays TJ, Rigby SP, Walker P, D'Ayala D (2007) Effects of carbonation on the pore structure of non-hydraulic lime mortars. Cement Concrete Res 37:1059–1069

Lubelli B, Van Hees RPJ, Huinink HP, Groot CJWP (2006) Irreversible dilation of NaCl contamined lime–cement mortar due to crystallization cycles. Cement Concrete Res 36:678–687

Maravelaki Kalaitzaki P, Bakolas A, Moropoulou A (2003) Physico-chemical study of Cretan ancient mortars. Cement Concrete Res 33:651–661

Martín JD (2004) XPowder. A software package for powder X-ray diffraction analysis. Lgl. Dep. GR 1001/04

Martínez Ramirez S, Puertas F, Blanco Varela MT, Thompson GE (1997) Studies on degradation of lime mortars in atmospheric simulation chambers. Cement Concrete Res 27:777–784

Martínez Ramirez S, Puertas F, Blanco Varela MT, Thompson GE (1998) Effect of dry deposition of pollutants on the degradation of lime mortars with sepiolite. Cement Concrete Res 28:125–133

Montoya C, Lanas J, Arandigoyen M, Navarro I, Garcia Casado PJ, Alvarez JI (2003) Study of ancient dolomitic mortars of the church of Santa Maria de Zamarce in Navarra (Spain): comparison with simulated standards. Thermochim Acta 398:107–122

Moreno F, Vilela SAG, Antunes ASG, Alves CAS (2006) Capillary-rising salt pollution and granitic stone erosive decay in the parish church of Torre del Moncorvo (NE Portugal). Implications for conservation strategy. J Cult Herit 7:56–66

Moropoulou A, Cakmak AS, Biscontin G, Bakolas A, Zendri E (2002) Advanced Byzantine cement based composites resisting earthquake stresses: the crushed brick/lime mortars of Justinian's Hagia Sophia. Constr Build Mat 16:543–552

Moropoulou A, Bakolas A, Anagnostopoulou S (2005) Composite materials in ancient structures. Cement Concrete Comp 27:295–300

Niesel K, Schimmelwitz P (1971) Hardening and weathering processes of dolomite lime mortars. Tonindustrie-Zeitung Keramische Rundschau 95:153–161

Pérez Bernal JL, Bello López MA (2004) Dióxido de azufre. Química atmosférica y destrucción del patrimonio. Fundación El Monte, Seville

Pérez Bernal JL, Bello López MA, Álvarez Gelindo JI (2004) The effect of relative humidity and foreign matter on the reaction between sulphur dioxide and calcium carbonate. In: Kwiatkowski D, Löfvendahl R (eds) Proceedings of the 10th international congress on deterioration and conservation of stone, vol 1. Stockholm (Sweden), pp 51–58

Price CA (1996) Stone conservation: an overview of current research. The Getty Conservation Institute, Los Angeles

Rodriguez-Navarro C, Dohene E (1999) Salt weathering: influence of evaporation rate, supersaturation and crystallization pattern. Earth Surf Proc Land 24:191–209

Rodriguez-Navarro C, Sebastian E (1996) Role of particulate matter form vehicle exhaust on porous building stones (limestone) sulfation. Sci Total Environ 187:79–91

Rodriguez-Navarro C, Hansen E, Ginell WS (1998) Calcium hydroxide crystal evolution upon aging of lime putty. J Am Ceram Soc 83:3032–3034

Rodriguez-Navarro C, Cazalla O, Elert K, Sebastian E (2002) Liesegang pattern development in carbonating traditional lime mortars. Proc R Soc London A 458:261–2273

Rodriguez-Navarro C, Ruiz-Agudo E, Ortega-Huertas M, Hansen E (2005) Nanostructure and irreversible colloidal behavior of $Ca(OH)_2$: implications in cultural heritage conservation. Langmuir 21:10948–10957

Ruiz-Agudo E (2007) Prevención del daño debido a la cristalización de sales en el patrimonio histórico construido mediante el uso de inhibidores de la cristalización. Ph.D. thesis, University of Granada

Ruiz-Agudo E, Mees F, Jacobs P, Rodriguez-Navarro C (2007a) The role of saline solution properties on porous limestone salt weathering by magnesium and sodium sulfates. Environ Geol 52:269–281

Ruiz-Agudo E, Martín Ramos JD, Rodríguez-Navarro C (2007b) Mechanisms and kinetics of dehydration of epsomite crystals formed in the presence of organic additives. J Phys Chem B 111:41–52

Sabbioni C, Zappia G, Gobbi G, Pauri MG (1993) Deterioration of ancient and modern building materials due to environmental factors. In: Brebbia CA, Frewer RJB (eds) Structural repair and maintenance of historical Buildings. Computational Mechanics Publications, Southampton, Boston, pp 235–242

Sabbioni C, Zappia G, Ghedini N, Gobbi G, Favoni O (1998) Black crusts on ancient mortars. Atmos Environ 32:215–223

Saiz Jiménez C, Brimblecombe P, Camuffo D, Lefèvre RA, Van Grieken R (2004) Damage caused to European monuments by air pollution: assessment and preventive measures. In: Air pollution and cultural heritage. Balkema Publishers, Rotterdam, pp 91–109

Siedel H (2000) Effects of salts on wall paintings and rendering in the Augustusburg Castle (Saxony). In: Proceedings of the 6th international congress on applied mineralogy, Göttingen, vol 2. Balkema, Rotterdam, pp 1035–1038

Simão J, Ruiz-Agudo E, Rodriguez-Navarro C (2006) Effects of particulate matter from gasoline and diesel vehicle exhaust emissions on silicate stones sulfation. Atmos Environ 40:6905–6917

Sunagawa I (1981) Characteristics of crystal growth in nature as seen from the morphology of mineral crystals. Bull Mineralogie 104:81–87

Tambe S, Gauri KL, Li S, Cobourn WG (1991) Kinetic study of SO_2 reaction with dolomite. Environ Sci Tech 25:2071–2075

Titiz Sargut S, Sayan P, Avci B (2007) Influence of citric acid on calcium sulfate dihidrate crystallization in aqueous media. Crystal Res Tech 42:119–126

Van Balen K (2005) Carbonation reaction of lime, kinetics at ambient temperature. Cement Concrete Res 35:647–657

Vecchio S, La Ginestra A, Frezza A, Ferragina C (1993) The use of thermoanalytical techniques in the characterization of ancient mortars. Thermochim Acta 227:215–223

Winkler EM (1973) Stone: properties, durability in man's environment. Springer, New York

Yates T (2003) Mechanism of air pollution damage to brick, concrete and mortar. In Brimblecombe P (ed) The effects of air pollution on the built heritage. Air pollution reviews, vol 2. Imperial College Press, London, pp 107–132

Zappia G, Sabbioni C, Pauri MG, Gobbi G (1992) Effect on SO_2-riched atmosphere on ancient and modern building materials. Mater Eng 3:445–458

Zappia G, Sabbioni C, Pauri MG, Gobbi G (1994) Mortar damage due to airborne sulfur compounds in a simulation chamber. Mater Struct 27:469–473